View Article Online
View Journal

Green Chemistry

Cutting-edge research for a greener sustainable future

Accepted Manuscript

This article can be cited before page numbers have been issued, to do this please use: K. Hatakeyama, Y. Nakagawa, M. Tamura and K. Tomishige, *Green Chem.*, 2020, DOI: 10.1039/D0GC01277G.

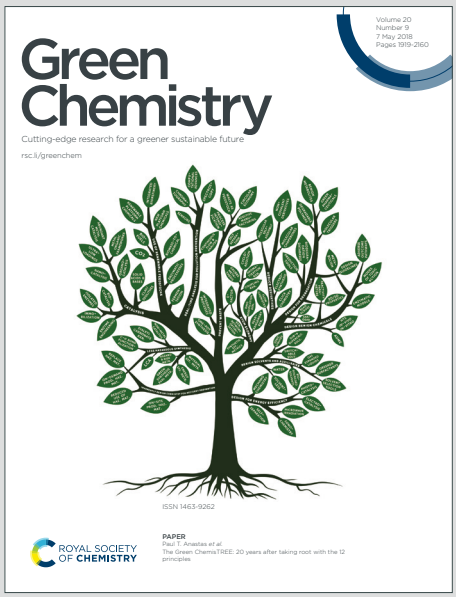

ROYAL SOCIETY OF CHEMISTRY

rsc.li/greenchem

View Article Online
DOI: 10.1039/D0GC01277G

Efficient production of adipic acid from 2-methoxycyclohexanone by aerobic oxidation with phosphotungstic acid catalyst

Kosuke Hatakeyama,[a] Yoshinao Nakagawa,[a,b,*] Masazumi Tamura,[a,b,†] and Keiichi Tomishige[a,b,*]

a Department of Applied Chemistry, School of Engineering, Tohoku University, Aoba 6-6-07, Aramaki, Aoba-ku, Sendai, 980–8579, Japan

b Research Center for Rare Metal and Green Innovation, Tohoku University, Aoba 468-1, Aramaki, Aoba-ku, Sendai, 980–0845, Japan

* Corresponding authors.

Yoshinao Nakagawa: yoshinao@erec.che.tohoku.ac.jp; tel&fax: +81-22-795-7215.

Keiichi Tomishige: tomi@erec.che.tohoku.ac.jp; tel&fax: +81-22-795-7214.

† Current address: Research Center for Artificial Photosynthesis, The Advanced Research Institute for Natural Science and Technology, Osaka City University, 3-3-138 Sugimoto, Sumiyoshi, Osaka, 558-8585, Japan

View Article Online
DOI: 10.1039/D0GC01277G

Abstract

Oxidative cleavage reaction of 2-methoxycyclohexanone (2-MCO) to adipic acid (AA) and methanol with O_2 in water solvent was investigated. 2-MCO and AA are one of lignin-based compounds produced via hydrogenation of guaiacol and an important monomer in industry, respectively. Various vanadium compounds and heteropolyacids were tested as homogeneous catalysts because vanadium compounds, especially phosphomolybdovanadic acids, have been known to be active in various oxidative cleavage reactions with O_2. Simple vanadium-free phosphotungstic acid ($H_3PW_{12}O_{40}$), which has not been regarded as an oxidation catalyst using O_2 as the oxidant, showed good catalytic activity and excellent selectivity to AA. The carbon-based AA yield reached 74% (86% in molar basis) and this value was higher than those obtained with vanadium-based catalysts. Reuse test and ^{31}P NMR confirmed that the $H_3PW_{12}O_{40}$ catalyst was stable and reusable. Kinetic studies and the reaction test using a radical inhibitor suggested that the reaction mechanism is not auto-oxidation involving free radicals. Instead, the substrate was first activated by one-electron oxidation by $H_3PW_{12}O_{40}$ catalyst and then reacted with O_2.

Keywords

Oxidative cleavage; Heteropolyacid; Biomass; Adipic acid

View Article Online
DOI: 10.1039/D0GC01277G

1. Introduction

Amid the concern of global warming and depletion of petroleum, which is indispensable in modern society as energy and source of chemicals, alternative resources for petroleum are being looked for. Biomass is attracting attention as one of alternative renewable resources to petroleum because biomass can be used for not only energy but also production of chemicals[1–7]. Among various types of biomass, woody biomass (lignocellulose) is valuable because it does not compete with human food production and exists in large quantity. Woody biomass mainly consists of cellulose, hemicellulose and lignin. While cellulose and hemicellulose are composed of sugar units and can be converted to similar compounds to those derived from edible biomass,[1-4] conversion of lignin has much different chemistry from that of cellulose, hemicellulose and edible biomass.[5-7] Lignin is expected as renewable raw material of cyclic compounds because lignin is a complex polyether of aromatics. In fact, fast pyrolysis of lignin (or woody biomass itself) can produce liquid compounds (bio-oil) which are available as source of energy and production of chemicals at high yield.[5,6] However, direct use of bio-oil is difficult because of the too much oxygen amount, instability and complex composition. So, researches on effective upgrading of bio-oil have been actively conducted.[7] Research on guaiacol conversion to useful compounds is one of them, such as phenol production using CoMo-,[8,9] Fe-,[10,11] Ni-,[12-15] Mo-[16-18] and ceria-[19] based catalysts and cyclohexanol production using Ru-,[20-23] Ni-,[24-27] Co-,[28] and Pt-[29] based catalysts. It is because guaiacol has the smallest molecule with three major types of C-O bonds in aromatic component of bio-oil (C_{aryl}-OH, C_{aryl}-OR and CH_3-O)[6,7] and because guaiacol itself is sometimes one of major component of bio-oil.[30,31] Synthesis of guaiacol by decarbonylation of vanillin, which is also a major component of bio-oil, has been reported.[32]

In this research, we focused on adipic acid, one of the most important monomers for

View Article Online
DOI: 10.1039/D0GC01277G

plastics[33], as a target product of guaiacol conversion. Adipic acid is currently produced from petroleum-based cyclohexane via the aerobic oxidation to K/A oil and further oxidation with nitric acid. Production of cyclohexane from renewable resources is not easy: typical method is isolation from total hydrodeoxygenation product of bio-oil which requires large amount of H_2 and difficulty in keeping the activity of hydrodeoxygenation catalyst. Guaiacol can be directly isolated from bio-oil, although the yield is not large, and it is an alternative source of renewable adipic acid. Conversion of guaiacol to adipic acid involves oxidation of 1 and 2 positions of carbon atoms in the phenol ring and hydrogen addition to 3, 4, 5 and 6 positions (Scheme 1). Therefore, the combination of hydrogenation and oxidation is necessary in this conversion. We select 2-methoxycyclohexanone (2-MCO) as the intermediate compound because 2-MCO is the simple product of hydrogenation of guaiacol at 3, 4, 5 and 6 positions (eq. (1)).

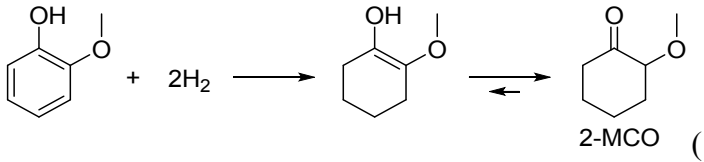

(1)

Pd catalysts are known to be effective in selective hydrogenation of phenols to cyclohexanones,[34] and that of guaiacol to 2-MCO has been actually reported with Pd/HAP catalyst.[35] Catalytic reduction of guaiacol to 2-MCO with formate as reducing agent has been also reported.[36] On the other hand, there are a number of studies on guaiacol hydrodeoxygenation to phenol, cyclohexanone or cyclohexanol.[8–29] Cyclohexanone and cyclohexanol can be oxidized to adipic acid with conventional nitric acid-based oxidation system.[37] Phenol can be easily hydrogenated to cyclohexanone or cyclohexanol. However, the production route of adipic acid via these monooxygenates from guaiacol consumes more amount of hydrogen (3 and 4 equiv. of H_2 for cyclohexanone and cyclohexanol

View Article Online
DOI: 10.1039/D0GC01277G

production, respectively), and in addition, it usually converts the methoxy group to less valuable methane, which requires further consumption of hydrogen. Other production routes of adipic acid from biomass typically use sugar-derived intermediates such as 2,5-furandicarboxylic acid[38-42] and sugar acids;[43-48] however, these routes require difficult and H_2-consuming (4 equiv. of H_2) hydrodeoxygenation to produce the tetramethylene group of adipic acid. Biological production of muconic acid or even adipic acid itself is possible,[49,50] and muconic acid can be converted to adipic acid by hydrogenation; however, these biological processes have not been established at a practical level. Other chemical production methods of adipic acid from biomass include extension of carbon chain from C5 intermediate compounds by (hydro)formylation,[51-54] carboxylation[55] and self-metathesis.[56] As an oxidative cleavage reaction of 2-MCO, Aakel et al. reported that phosphomolybdovanadic acid $H_6PV_3Mo_9O_{40}$ catalyzes the oxidation of 2-MCO with O_2 in methanol solvent into dimethyl adipate (eq. (2)) in 52% mol-based yield.[57] On the other hand, use of nonflammable water solvent (eq. (3)) is more desirable from the viewpoint of safety, and in addition, free adipic acid can be easily crystallized or extracted from water solvent.

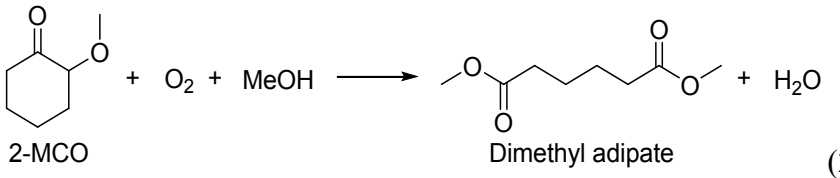

(2)

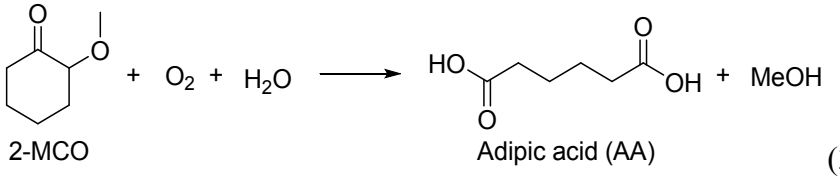

(3)

However, oxidation of 2-MCO with O_2 to free adipic acid has not been reported in the literature, to the best of our knowledge. Here, we develop catalytic systems for eq. (3). First, we tested vanadium-

View Article Online
DOI: 10.1039/D0GC01277G

based catalysts because they are known to be effective in oxidative cleavage reaction of a related compound 2-hydroxycyclohexanone (2-HCO).[57-62] We also explored heteropolyacids as catalysts because phosphomolybdovanadic acid is one of heteropolyacids and the redox properties of heteropolyacids and their salts (polyoxometalates) can be controlled at molecular level.[63,64] Surprisingly, we found that vanadium-free $H_3PW_{12}O_{40}$ is an effective catalyst in this reaction, in contrast to the general knowledge that $H_3PW_{12}O_{40}$ is not an oxidation catalyst with O_2 as an oxidant.

2. Experimental

2.1. Catalyst

V_2O_5 was purchased from Wako. $H_5PV_2Mo_{12}O_{40}\cdot 25H_2O$ was purchased from Nippon Inorganic Colour & Chemical Co., Ltd. $H_3PMo_{12}O_{40}\cdot nH_2O$ (n=21 as determined by thermogravimetric and differential thermal analysis (TG-DTA)) was purchased from Tokyo Chemical Industry Co., Ltd. $H_3PW_{12}O_{40}\cdot nH_2O$ (n=10 as determined by TG-DTA) was purchased from Yoneyama Yakuhin Kogyo Co., Ltd. $H_4SiW_{12}O_{40}\cdot 26H_2O$ and $Na_3PW_{12}O_{40}\cdot nH_2O$ (n=13 as determined by TG-DTA) were purchased from Nakalai Tesque, Inc. H_2WO_4 was purchased from Strem Chemicals, Inc. $H_4PVW_{11}O_{40}$ was synthesized by the following method based on the literature:[65] 5 g of $NaVO_3$ (dissolved in 50 ml of 0.91 M aqueous oxalic acid) and 3 g of Na_2HPO_4 (dissolved in 50 ml of distilled water) were mixed. 50 g of $Na_2WO_4\cdot 2H_2O$ (dissolved in 150 ml of distilled water) was added, then the mixed solution was heated to 353 K and then 30 ml of concentrated H_2SO_4 was slowly added to the solution. The solution was stirred for 8 h. After cooling the solution to room temperature, $H_4PVW_{11}O_{40}$ was extracted with diethyl ether from the solution. The solvent was evaporated to obtain a solid product which was washed with distilled water and dried. ^{31}P and ^{51}V NMR was measured with Bruker AV400 instrument. Phosphoric acid and $SiVW_{11}O_{40}^{5-}aq$ were used as external standards

View Article Online
DOI: 10.1039/D0GC01277G

(0 ppm (^{31}P) and -550 ppm (^{51}V), respectively). Aqueous solution of reduced phosphotungstic acid ($H_{4.3}PW_{12}O_{40}$) was prepared by the following method: $H_3PW_{12}O_{40}$ (220 μmol) was dissolved in water (20 g). Pt/C (5 wt% Pt, Wako, 67 mg) was added, and the mixture was treated with 1 MPa of H_2 at room temperature in an autoclave for 1 h. The solution of reduced phosphotungstic acid was collected by filtering out the Pt/C catalyst under N_2. The reduction degree was determined by titration with aqueous $Ce(NH_4)_4(SO_4)_4$ until the deep blue color of the reduced heteropolyanion disappeared ($xCe^{4+} + H_{3+x}PW_{12}O_{40} \rightarrow xCe^{3+} + H_3PW_{12}O_{40} + xH^+$).

2.2. Activity tests

The oxidation reaction was performed in a 190 mL stainless-steel autoclave with an inserted glass vessel. The catalyst, substrate, and water (10 mL) were put into the autoclave together with a spinner. All the catalysts in this study are soluble in water (homogeneous system). The pH was measured by using a pH meter if necessary. After sealing, the reactor was filled with 0.8 MPa O_2 (at r. t.). The autoclave was heated to 353 K, which took about 40 min to reach, and the temperature was monitored by using a thermocouple inserted in the autoclave. The stirring rate was fixed at 500 rpm (magnetic stirring). After an appropriate reaction time, the reactor was cooled by a cold water bath, and the gases were collected in a gas bag. The autoclave contents, sometimes containing adipic acid crystals, were diluted/dissolved with 2-propanol and transferred to a vial. If catalyst-derived solid was formed it was separated by filtration through a membrane filter. The liquid phase was analyzed by using HPLC (Shimadzu Prominence; Aminex HPX-87 H column (Bio-Rad), 0.01 M sulfuric acid as eluent, UV detector (210 nm) and RID). 1,6-Hexanediol was used as internal standard which was added after reaction. The gas phase was analyzed by using GC with flame ionization detection (FID) and methanator (Shimadzu GC-2014, Porapak N packed column). External standard method was used for

View Article Online
DOI: 10.1039/D0GC01277G

gas phase analysis, and the analysis was repeated to exclude the failure in sampling. The formation of adipic acid was also confirmed by ^{1}H NMR of the reaction mixture using D_2O as solvent (Fig. S1). The conversion, selectivity, yield and carbon balance were calculated from the following formulas: Conversion [%]=(mol of consumed substrate)/(mol of charged substrate)×100; Selectivity [%-C]=[(mol of product)×(number of carbon atoms in the product)]/[(mol of consumed substrate)×(number of carbon atoms in the substrate)]×100; Yield [%-C]=[(mol of product)×(number of carbon atoms in the product)]/[(mol of charged substrate)×(number of carbon atoms in the substrate)]×100; Carbon balance [%]=Σ[(mol of compound)×(number of carbon atoms in the compound)]/[(mol of charged substrate)×(number of carbon atoms in the substrate)]×100. We used carbon-based selectivity and yield because the oxidative dissociation including CO_2 formation increases the number of molecules and the sum of mol-based selectivities does not become 100%. Mol-based yield of adipic acid [%], defined as [mol of adipic acid]/[mol of charged 2-MCO]×100, can be calculated by the following formula: (carbon-based yield of adipic acid [%-C])×7/6. Similarly, mol-based yield of methanol [%] can be calculated by (carbon-based yield of methanol [%-C])×7.

3. Result and discussion

3.1. Catalyst survey

Table 1 lists the results of the catalyst screening for the oxidation of 2-methoxycyclohexanone (2-MCO). Theoretical maximum yield of adipic acid (AA) was 86% because product yield was calculated on carbon basis. First, we tested vanadium catalysts which have been reported to be active in oxidative cleavage reactions of various substrates such as hydroxyketones,[57-62] carbohydrates,[66-74] catechols,[75-77] lignin and lignin-model compounds,[78-83] malic acid[84] and 5-hydroxymethylfurfural.[85] $H_5PV_2Mo_{10}O_{40}$ system, which is a typical vanadium-based oxidation

View Article Online
DOI: 10.1039/D0GC01277G

catalyst[63,64] and showed good performance in the previous report for 2-MCO oxidation to dimethyl adipate[57], showed high conversion; however, AA yield was low (entry 2) and in addition the reaction stopped before complete conversion of 2-MCO (Fig. S2). V_2O_5 catalyst, which is the simplest vanadium catalyst, showed low AA yield even at high conversion level (entries 3 and 4). Various by-products including shorter-chain dicarboxylic acids, formic acid and CO_2 were observed with these two vanadium catalysts. Next, we explored the catalysts of the combination of vanadium species and heteropolyacids. Addition of $H_3PMo_{12}O_{40}$ to V_2O_5 greatly increased the conversion and AA selectivity, especially by suppression of shorter-chain dicarboxylic acid and formic acid (entry 5). Addition of $H_3PW_{12}O_{40}$ to V_2O_5 also greatly increased the conversion and slightly increased the AA selectivity (entry 6). Addition of $H_4SiW_{12}O_{40}$ to V_2O_5 greatly increased the conversion, while the AA selectivity decreased (entry 7). Although addition of $H_3PMo_{12}O_{40}$ showed the highest AA yield, it is known that various types of vanadium species and polyoxometalates are formed in the mixed solution of vanadium and $H_3PMo_{12}O_{40}$,[63,64] making it difficult to discuss the true active species. We are interested in the good result of V_2O_5 + $H_3PW_{12}O_{40}$ system because $H_3PW_{12}O_{40}$ has been hardly used as oxidation catalyst using O_2 as an oxidant.[86] In fact, $H_3PW_{12}O_{40}$ was reported to be inactive in oxidation of malic acid[84] and 5-hydroxymethylfurfural[85] with O_2 in organic solvent in the conditions where $H_5PV_2Mo_{10}O_{40}$ showed good activity. We tested $H_4PVW_{11}O_{40}$ and $H_3PW_{12}O_{40}$ as catalysts (entries 8 and 9) because we considered that the formation of $H_4PVW_{11}O_{40}$ might be a cause of increase of AA yield in V_2O_5 + $H_3PW_{12}O_{40}$ system. $H_4PVW_{11}O_{40}$ catalyst system showed similar conversion to that in V_2O_5 + $H_3PW_{12}O_{40}$ system and much higher AA selectivity than that in V_2O_5 + $H_3PW_{12}O_{40}$ system (entry 8). However, interestingly, $H_3PW_{12}O_{40}$ alone system showed the highest AA selectivity and relatively high conversion (entry 9). The reactions with other typical heteropolyacids were also carried out. $H_4SiW_{12}O_{40}$ alone system also showed activity (entry 10).

View Article Online
DOI: 10.1039/D0GC01277G

However, the conversion and AA selectivity were lower than that of $H_3PW_{12}O_{40}$. $H_3PMo_{12}O_{40}$ and $H_4SiMo_{12}O_{40}$ alone systems showed similar activity of $H_3PW_{12}O_{40}$ system (Table S1, entries 10 and 11). The color of the reaction solution with $H_3PMo_{12}O_{40}$ or $H_4SiMo_{12}O_{40}$ became black or green (Fig. S3 (b) and (c)), which indicated the reduction of heteropolyacid, while in the case of $H_3PW_{12}O_{40}$ the reaction solution remained colorless (Fig. S3 (a)). Therefore, we further investigated the $H_3PW_{12}O_{40}$ system because of the simplicity and easy characterization of the catalyst. In addition, elution effect of metal species from the wall of autoclave (stainless steel) in $H_3PW_{12}O_{40}$ system was checked because in our autoclave a stainless steel sheath for thermocouple contacted with the reaction solution. When the sheath was covered with a teflon tube to avoid the direct contact between the reaction solution and stainless steel, the reaction result was not changed (Table S1, entry 8). The reaction with H_2WO_4 as catalyst showed almost no activity (entry 11). The reaction with H_2SO_4 showed that small amount of AA was formed with a simple acid catalyst (entry 12). However, the activity and selectivity were much lower than the case of $H_3PW_{12}O_{40}$ catalyst. The results of these control experiments suggest that $H_3PW_{12}O_{40}$ was actually an active catalyst in the 2-MCO oxidation to AA with O_2 (eq. (3)). Methanol was formed almost stoichiometrically (carbon-based yield with about 1/7 of the conversion value), and the formation of CO_2 was negligible in the $H_3PW_{12}O_{40}$ catalyst system. The small formation of CO_2 is characteristic to the $H_3PW_{12}O_{40}$ catalyst system, which contrasts with the vanadium-based C–C cleavage reaction systems where significant amount of CO_2 was formed.[61,62,66-74] The higher selectivity of $H_3PW_{12}O_{40}$ catalyst than other catalysts in Table 1 is further confirmed by comparing the conversion-AA yield dependency of $H_3PW_{12}O_{40}$ catalyst obtained in later sections with each entry in Table 1 data (Fig. S4). All the other catalysts in Table 1 showed lower adipic acid yield than $H_3PW_{12}O_{40}$ catalyst at the same conversion level.

View Article Online
DOI: 10.1039/D0GC01277G

3.2. Optimization of reaction conditions

3.2.1. Effect of the oxygen pressure

First, the results of the reactions under different oxygen pressures are shown in Table 2. In the range of O_2 pressure of 0.1–0.8 MPa, the conversion and AA selectivity were almost unchanged (entries 1–4). These results indicated the zero-order dependence on oxygen pressure in this range, suggesting that the steps involving O_2 molecule were fast. Nevertheless, the AA yield was very slightly larger under higher O_2 pressure. We selected 0.8 MPa O_2 as the standard condition.

When the reaction was carried out without O_2 (at zero O_2 pressure), the conversion of 2-MCO was much lower than the cases with O_2 and a small amount of 2-HCO was detected as the hydrolysis product (entry 5; eq. (4)). The color of reaction solution was changed to black, which indicates the reduction of $H_3PW_{12}O_{40}$ (Fig. S3 (d)). The reduction degree of the heteropolyacid (x in $H_{3+x}PW_{12}O_{40}$) after the 24 h reaction without O_2 was determined by titration with Ce^{4+}. The determined x value was 0.37, which means that more than 60% of the heteropolyacid remained in the fully oxidized state ($H_3PW_{12}O_{40}$). At shorter reaction time (6 h), the reduction degree of the heteropolyacid was x=0.21, which was lower than that at 24 h. These data indicated that the reduction of $H_3PW_{12}O_{40}$ to free $H_4PW_{12}O_{40}$ proceeded very slowly under O_2-free conditions. The role of 2-HCO and reduced heteropolyacid in the reaction mechanism will be discussed later.

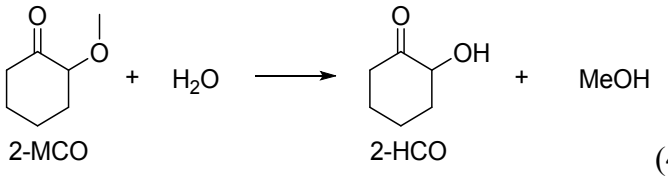

(4)

3.2.2. Effect of the reaction temperature

The results of the reactions at different reaction temperature (323–383 K) are shown in Table

View Article Online
DOI: 10.1039/D0GC01277G

3. The reaction proceeded very slowly at 323 K and the conversion was low even after long reaction time (entries 1 and 2). At 353 K, the conversion increased to almost 100% at longer reaction time with keeping high AA selectivity (entries 3 and 4). At 383 K, the activity was further increased; however, the AA selectivity was decreased (entry 5). We selected 353 K as the standard reaction temperature.

3.2.3. Effect of the ratio of $[H^+]$ and $[PW_{12}O_{40}^{3-}]$

The reactions in different ratio of $[H^+]$ and $[PW_{12}O_{40}^{3-}]$ were conducted to investigate the effect of their concentrations because $H_3PW_{12}O_{40}$ was ionized to H^+ and $PW_{12}O_{40}^{3-}$ in water solution. The ratio of $[H^+]$ and $[PW_{12}O_{40}^{3-}]$ was adjusted by using H_2SO_4 as H^+ component and $Na_3PW_{12}O_{40}$ as $PW_{12}O_{40}^{3-}$ component. The results are shown in Fig. 1. The conversion was improved by addition of H^+ to $Na_3PW_{12}O_{40}$ and was increased with the increase of H^+ amount. The conversion was also improved by addition of $PW_{12}O_{40}^{3-}$ and was increased with the increase of $PW_{12}O_{40}^{3-}$ amount. These results indicated that both H^+ and $PW_{12}O_{40}^{3-}$ were involved in the catalysis. The reaction results using different amount of $H_3PW_{12}O_{40}$ are shown in Fig. S5. The conversion and AA yield were increased linearly with the increase of catalyst amount, which suggests the first-order dependence on $H_3PW_{12}O_{40}$ amount. The initial TOF of AA production calculated by the slope was 0.8 h^{-1}.

3.2.4. Time course of oxidation with $H_3PW_{12}O_{40}$

Time course of the 2-MCO oxidation with $H_3PW_{12}O_{40}$ as catalyst is shown in Fig. 2. The conversion at 0 h means the reaction during the heating from room temperature to target one which took about 1 h. The conversion increased with time and reached almost 100% at 120 h. The highest yield of AA (74%-C) was obtained at this time (same data of Table 3, entry 4). The mol-based yield

View Article Online
DOI: 10.1039/D0GC01277G

of AA was 86% and this value is much higher than the diester yield in the previous report (52%).[57] The TON of AA production at the condition with the highest yield was 34.

The relationship between $\ln(C_{2\text{-MCO}}/C_0)$ ($C_{2\text{-MCO}}$: concentration of 2-MCO after reaction, C_0: initial concentration of 2-MCO) and time (Fig. S6) showed a straight line through the origin. This result suggests the first-order reaction with respect to 2-MCO concentration.

3.2.5. Reusability of $H_3PW_{12}O_{40}$

The reuse experiment of $H_3PW_{12}O_{40}$ catalyst was carried out. Because $H_3PW_{12}O_{40}$ is a homogeneous catalyst and the solubility of AA is not large in cold water, the following method was applied to the reuse test: The solution after reaction was cooled to 273 K, the precipitated AA was collected by filtration (the collected AA yield was about 30%-C), 2-MCO was added in the consumed amount to the solution to the original concentration level, and the next run was conducted. The yield and selectivity were calculated based on the increase of the amount of each product. The results are shown in Fig. 3. The conversion and AA selectivity hardly changed during the reuse experiment. The data also indicate no formation of insoluble solid derived from catalyst such as tungsten bronze. In addition, ^{31}P NMR of the reaction solution after the reuse experiment was measured to investigate whether $H_3PW_{12}O_{40}$ maintained the polyoxometalate structure. As shown in Fig. 4, the ^{31}P NMR signal of $PW_{12}O_{40}^{3-}$ was not changed, indicating that decomposition of Keggin structure or formation of lacunary polyoxometalates did not proceed during the catalysis. These data indicated that $H_3PW_{12}O_{40}$ was a stable and reusable catalyst. The reusability of the $H_3PW_{12}O_{40}$ solution suggests the potential of semi-batch process with continuous feeding of 2-MCO and removal of adipic acid.

3.3. Reaction mechanism

View Article Online
DOI: 10.1039/D0GC01277G

3.3.1. Kinetics

As described above, the reaction order with respect to O_2 and 2-MCO concentration were determined to be zero and suggested to be one, respectively. To confirm the first-order dependence on 2-MCO concentration, the reactions in different substrate amount were carried out. As shown in Fig. 5, the conversion values were similar in the reactions in up to 0.43 mol/L 2-MCO concentration range at the same reaction time. These results indicated that the converted amount was proportional to the 2-MCO concentration. However, at 0.86 mol/L 2-MCO the conversion value became lower. These data showed that at lower 2-MCO concentrations (≤ 0.43 mol/L) the reaction order with respect to 2-MCO concentration was one, while at higher concentration the reaction order was lower.

3.3.2. Application to related substrates

The $H_3PW_{12}O_{40}$ catalyst system was applied to various related substrates, and the results are shown in Tables 4 and 5. The reaction of guaiacol hardly proceeded (Table 4, entry 2). Next, the reaction of 2-HCO was conducted because 2-HCO may be an intermediate in the reaction of 2-MCO (Table 4, entries 3–5). The dependence of 2-HCO concentration was also investigated because 2-HCO concentration in the reaction of 2-MCO should be very low. Although the conversion of 2-HCO was very high, the AA selectivity was low and did not depend on the concentration. These results indicated that 2-HCO was not an intermediate and AA was produced by direct cleavage of 2-MCO. The reactions of *trans*-1,2-cyclohexanediol, cyclohexanone and methoxycyclohexane hardly proceeded (Table 4, entries 6–8). The presence of both ketone and methoxy/hydroxyl groups was essential in the reactivity. In addition, the reactions of 3-hydroxy-2-butanone, hydroxyacetone, methoxyacetone and methoxyacetic acid which have both of ketone and hydroxyl/methoxy groups were tested (Table 5). The reaction of 3-hydroxy-2-butanone proceeded to some extent and 48%-C

View Article Online
DOI: 10.1039/D0GC01277G

yield of acetic acid was obtained (Table 5, entry 1). While the reaction of hydroxyacetone also proceeded to some extent, the conversion was low and selectivities to target products (formic acid and acetic acid) were not high (Table 5, entry 2). The reactivity of methoxyacetone was lower than that of hydroxyacetone (Table 5, entry 3 and 4); while the selectivities to target products (formic acid and acetic acid as well as methanol derived from the methoxy group) were higher than the case of the reaction of hydroxyacetone. These lower reactivities and higher selectivities of methoxyacetone than hydroxyacetone were similar to the case of 2-MCO/2-HCO. The reaction of methoxyacetic acid did not proceed at all (Table 5, entry 5). These results indicated that $H_3PW_{12}O_{40}$ catalyst system is effective to the oxidative C–C cleavage of α-methoxyketones and less effective to that of α-hydroxyketones.

3.3.3. Effect of the addition of radical inhibitor

The addition of 2,6-di-*tert*-butyl-*p*-cresol as a radical inhibitor to 2-MCO oxidation with $H_3PW_{12}O_{40}$ was tested to determine whether or not this oxidation proceeds by auto-oxidation mechanism where free organic radicals unbound from catalyst react with another substrate molecule and/or O_2 biradical. As shown in Table 6, addition of radical inhibitor did not affect both conversion and selectivity (entries 2 and 3). This result suggested another mechanism than auto-oxidation involving free radicals.

3.3.4. Reactivity of reduced heteropolyacid

The reduced form of aqueous $H_3PW_{12}O_{40}$ ($H_{4.3}PW_{12}O_{40}$) was synthesized by reduction of $H_3PW_{12}O_{40}$ solution with Pt/C catalyst and H_2. The solution was used for oxidation of 2-MCO under standard reaction conditions (0.8 MPa O_2). The "heteropoly blue" color disappeared even when the

View Article Online
DOI: 10.1039/D0GC01277G

solution was heated to the reaction temperature (353 K), and the reaction result after 24 h was essentially the same to the standard run with $H_3PW_{12}O_{40}$ catalyst (Table 6, entry 4). The ^{31}P NMR of the reaction solution of reduced heteropolyacid catalyst showed preservation of the structure of $PW_{12}O_{40}^{3-}$. These data mean that the $H_3PW_{12}O_{40}$ catalyst can be easily reoxidized with O_2 even when reduced. On the other hand, as described in section 3.2.1, the amount of reduced heteropolyacid was increased very slowly under O_2-free conditions: x=0.21 and 0.37 as $H_{3+x}PW_{12}O_{40}$ at 6 h and 24 h, respectively. This means that only 1-3% of $H_3PW_{12}O_{40}$ was reduced to $H_4PW_{12}O_{40}$ per 1 h reaction with substrate. The reaction rate was much lower than the TOF value (0.8 h^{-1}) of AA formation in the standard reaction conditions. This difference indicates that direct involvement of free reduced heteropolyacid ($H_4PW_{12}O_{40}$) in the reaction cycle is not plausible. The formation of free $H_4PW_{12}O_{40}$ is a side reaction in the oxidation of 2-MCO to AA; however, this reaction is not a large problem because it is much slower than the main reaction and the formed reduced $H_4PW_{12}O_{40}$ is rapidly reoxidized with O_2 in the standard reaction conditions.

3.3.5. Proposed reaction mechanism

The reaction kinetics showed that the reaction orders with respect to $H_3PW_{12}O_{40}$ catalyst, 2-MCO and O_2 were one, one and zero, respectively (section 3.3.1). These kinetics suggest that the 2-MCO is first activated by the reaction with $H_3PW_{12}O_{40}$ catalyst, and this is the rate-determining step. The activated substrate then reacts with O_2. Considering the high reactivity of the intermediate with O_2, we think that the radical formed by one-electron oxidation of 2-MCO with $H_3PW_{12}O_{40}$ is the intermediate. However, as discussed in section 3.2.1 and 3.3.4, the formation of dissolved reduced heteropolyanion ($PW_{12}O_{40}^{4-}$) as a free form is very slow. We think that the activated substrate radical is attached to $PW_{12}O_{40}^{4-}$ formed by the one-electron reduction. However, there is no strong interaction

View Article Online
DOI: 10.1039/D0GC01277G

between heteropolyanion and neutral radical. The softness of heteropolyacids can be a key; heteropolyanions have general ability to stabilize organic cations, which is assumed to play an important role in the organic reactions.[63] We think that the radical cation which is first formed by electron abstraction from the substrate is stabilized and involved in the catalysis. The proposed reaction mechanism is shown in Fig. 6. First, 2-MCO is oxidized by one-electron by $H_3PW_{12}O_{40}$ to the radical cation of the enol form of 2-MCO (step (i)). This is the rate-determining step. The organic cation is paired with $PW_{12}O_{40}^{4-}$ based on the softness of heteropolyanions. The acidity of the reaction media is necessary to form the organic cation. The pairing with reduced $PW_{12}O_{40}^{4-}$ can decrease the reactivity of the radical with radical inhibitor which is a one-electron reducing agent. On the other hand, the radical cation can have high reactivity with one-electron oxidant. Then, O_2 is added to the carbon atom bonded with the methoxide group (step (ii)). The formed superoxide radical rapidly reacts with the reduced heteropolyacid ($H_4PW_{12}O_{40}$), which has been attached to the activated substrate, to form the hydroperoxide and oxidized $H_3PW_{12}O_{40}$ (step (iii)). This step is a kind of intramolecular process, and it is faster than the reaction of the superoxide radical with an externally added radical inhibitor, leading to the absence of addition effect of radical inhibitor (section 3.3.3). The C–C bond in vicinal hydroperoxo keto structure is cleaved by Grob-type fragmentation (step (v)) after addition of water to keto group (step (iv)).[87] The dissociation of C-C bond concerted with O-O cleavage of connected peroxo group via Grob-type fragmentation has been reported for Fe- and Cu-catalyzed systems.[88-90] Monomethyl adipate is formed by the fragmentation, and it is easily hydrolyzed in acidic water to form final product adipic acid (step (vi)). In this mechanism, the key step is clearly the formation of radical cation (step (i)). In the case of 2-HCO oxidation, the product of step (iii) is 2-hydroxy-2-hydroperoxycyclohexanone which can be decomposed to 1,2-cyclohexanedione and H_2O_2. The large amount of by-products in 2-HCO oxidation can be derived

View Article Online
DOI: 10.1039/D0GC01277G

from oxidation of 1,2-cyclohexanedione. We carried out DFT calculation of the formation energy of radical cation of various molecules, i.e. energy change by one-electron oxidation (Table 7). The radical cation of the enol form of 2-MCO can be favorably formed, according to the low ΔE (+694 kJ mol^{-1}). This value is even lower than that of 2,6-di-*tert*-butyl-*p*-cresol (+706 kJ mol^{-1}) which is a well-known one-electron reducing agent and works as a radical inhibitor. The calculated low formation energy of radical cation supported the involvement of the radical cation in the oxidation catalysis. The calculated structure of the radical cation of 2-methoxycyclohexanone is shown in Fig. 7. The cation is stabilized by the electron-donating –OH and –OCH_3 groups. The unpaired electron is mainly present as $\pi_{C–C}$ bond (Fig. 7, (b)), and O_2 will attack the unpaired π electron to form a C–O bond.

4. Conclusions

$H_3PW_{12}O_{40}$ can selectively convert 2-methoxycyclohexanone (2-MCO) to adipic acid (AA) and methanol with O_2 as an oxidant in water solvent. The carbon-based yield of AA reached 74%-C. The mol-based yield of AA was 86% and this value is much higher than the diester yield in a previous report[47] using phosphomolybdovanadic acid catalyst and methanol solvent (52%). Vanadium catalysts such as V_2O_5 and phosphomolybdovanadic acid in our conditions using water solvent showed lower selectivity to AA. Significant amount of CO_2 was produced with both vanadium-based catalysts because of the high activity of vanadium as oxidation catalysts. In addition, catalyst deactivation was observed for phosphomolybdovanadic acid. In contrast, the $H_3PW_{12}O_{40}$ catalyst was stable during the reuse experiment. The produced AA was easily separated from the reaction solution by crystallization. This catalytic system is also active in the oxidative cleavage of α-hydroxyketones; however, the selectivity to the corresponding acids is lower than the case of α-methoxyketones.

View Article Online
DOI: 10.1039/D0GC01277G

Cyclohexanone (a simple ketone), methoxycyclohexane (a simple methoxide), *trans*-1,2-cyclohexanediol (a vicinal diol), guaiacol and methoxyacetic acid (an α-methoxycarboxylic acid) are not reactive. The catalysis followed the kinetics of first orders on substrate (2-MCO) and catalyst ($H_3PW_{12}O_{40}$) concentrations and zero order on O_2 pressure. These kinetics suggest that the substrate is first activated on the catalyst as the rate-determining step and then reacts with O_2 molecule. The mechanism which is different from typical auto-oxidation involving free radicals is also supported by the negligible effect of the addition of radical inhibitor (2,6-di-*tert*-butyl-*p*-cresol) to the system. We propose that the first step is the one-electron oxidation of 2-MCO with $PW_{12}O_{40}^{3-}$ to form the ion pair of radical cation of the enol form of 2-MCO and $PW_{12}O_{40}^{4-}$, considering that 2-hydroxycyclohexanone (2-HCO; hydrolysis product of 2-MCO) and free $PW_{12}O_{40}^{4-}$ are suggested not to be intermediates. This new reaction not only enables efficient and safe production of AA with minimum amount of H_2 from biomass but also enlarges the catalytic chemistry using heteropolyacids.

Conflicts of interest

There are no conflicts of interest to declare.

Acknowledgement

This work is supported by JSPS KAKENHI 18H05247.

References

1. A. Corma, S. Iborra and A. Velty, *Chem. Rev.* 2007, **107**, 2411–2502.

2. M. Besson, P. Gallezot and C. Pinel, *Chem. Rev.* 2014, **114**, 1827–1870.

3. L.T. Mika, E. Cséfalvay and Á. Németh, *Chem. Rev.* 2018, **118**, 505–613.

View Article Online
DOI: 10.1039/D0GC01277G

4. B.M. Stadler, C. Wulf, T. Werner, S. Tin and J.G. de Vries, *ACS Catal*. 2019, **9**, 8012−8067.

5. W. Mu, H. Ben, A. Ragauskas and Y. Deng, *Bioenerg. Res.* 2013, **6**, 1183–1204.

6. H. Wang, J. Male and Y. Wang, *ACS Catal*. 2013, **3**, 1047–1070.

7. L. Yang, K. Seshan and Y. Li, *Catal. Today* 2017, **298**, 276–297.

8. I. D. Mora, E. Mendez, L.J. Duarte and S.A. Giraldo, *Appl. Catal. A Gen.* 2014, **474**, 59–68.

9. E. Laurent and B. Delmon, *Appl. Catal. A Gen.* 1994, **109**, 77–96.

10. J. Sun, A.M. Karim, H. Zhang, L. Kovarik, X.S. Li, A.J. Hensley, J.-S. McEwen and Y. Wang, *J. Catal*. 2013, **306**, 47–57.

11. R. Olcesea, M.M. Bettaharb, B. Malamanc, J. Ghanbajac, L. Tibavizcoa, D. Petitjeana and A. Dufour, *Appl. Catal. B Environ.* 2013, **129**, 528–538.

12. S.-K. Wu, P.-C. Lai, Y.-C. Lin, H.-P. Wan, H.-T. Lee and Y.-H. Chang, *ACS Sustain. Chem. Eng.* 2013, **1**, 349–358.

13. S.T. Oyama, T. Onkawa, A. Takagaki, R. Kikuchi, S. Hosokai, Y. Suzuki and K.K. Bando, *Top. Catal.* 2015, **58**, 201–210.

14. Z. Cai, F. Wang, X. Zhang, R. Ahishakiye, Y. Xie and Y. Shen, *Mol. Catal.* 2017, **441**, 28–34.

15. X. Zhang, P. Yan, B. Zhao, K. Liu, M.C. Kung, H.H. Kung, S. Chen and Z.C. Zhang, *ACS Catal.* 2019, **9**, 3551–3563.

16. C. Sepúlveda, K. Leiva, R. García, L.R. Radovic, I.T. Ghampson, W.J. DeSisto, J.L. García Fierro and N. Escalona, *Catal. Today* 2011, **172**, 232–239.

17. Z. Cao, J. Engelhardt, M. Dierks, M.T. Clough, G.-H. Wang, E. Heracleous, A. Lappas, R. Rinaldi and F. Schüth, *Angew. Chem. Int. Ed.* 2017, **56**, 2334–2339.

18. S. Liu, H. Wang, K.J. Smith and C.S. Kim, *Energy Fuels* 2017, **31**, 6378–6388.

19. S.M. Schimming, O.D. LaMont, M. Köng, A. Rogers, A.D. D'Amico, M.M. Yung and C. Sievers,

View Article Online
DOI: 10.1039/D0GC01277G

ChemSusChem 2015, **8**, 2073–2083.

20. Y. Nakagawa, M. Ishikawa, M. Tamura and K. Tomishige, *Green Chem.* 2014, **16**, 2197–2203.

21. M. Ishikawa, M. Tamura, Y. Nakagawa and K. Tomishige, *Appl. Catal. B* 2016, **182**, 193–203.

22. G.-Y. Xu, J.-H. Guo, Y.-C. Qu, Y. Zhang, Y. Fu and Q.-X. Guo, *Green Chem.* 2016, **18**, 5510–5517.

23. M.A. Gonzalez-Borja and D.E. Resasco, *Energy Fuels* 2011, **25**, 4155–4162.

24. J. Long, S. Shu, Q. Wu, Z. Yuan, T. Wang, Y. Xu, X. Zhang, Q. Zhang and L. Ma, *Energy Conv. Manag.* 2015, **105**, 570–577.

25. M. Zhou, Y. Wang, Y. Wang and G. Xiao, *J. Energy Chem.* 2015, **24**, 425–431.

26. W. Schutyser, G. Van den Bossche, A. Raaffels, S. Van den Bosch, S.-F. Koelewijn, T. Renders and B.F. Sels, *ACS Sustainable Chem. Eng.* 2016, **4**, 5336−5346.

27. J. Feng, Z. Yang, C.-Y. Hse, Q. Su, K. Wang, J. Jiang and J. Xu, *Renew. Energy* 2017, **105**, 140–148.

28. X. Liu, W. Jia, G. Xu, Y. Zhang and Y. Fu, *ACS Sustain. Chem. Eng.* 2017, **5**, 8594–8601.

29. M. Kim, J.-M. Ha, K.-Y. Lee and J. Jae, *Catal. Commun.* 2016, **86**, 113–118.

30. J.-S. Kim, *Bioresource Technol.* 2015, **178**, 90–98.

31. D. K. Shen, S. Gu, K. H. Luo, S. R. Wang and M. X. Fang, *Bioresource Technol.* 2010, **101**, 6136–6146.

32. Y.-B. Huang, Z. Yang, M.-Y. Chen, J.-J. Dai, Q.-X. Guo and Y. Fu, *ChemSusChem* 2013, **6**, 1348–1351.

33. S. Van de Vyver and Y. Román-Leshkov, *Catal. Sci. Technol.* 2013, **3**, 1465–1479.

34. Y. Shao, J. Zhang, Y. Du, H. Jiang, Y. Liu and R. Chen, *Ind. Eng. Chem. Res.* 2019, **58**, 14678–14678–14687.

View Article Online
DOI: 10.1039/D0GC01277G

35. G. Xu, J. Guo, Y. Zhang, Y. Fu, J. Chen, L. Ma and Q. Guo, *ChemCatChem* 2015, **7**, 2485–2492.

36. F. Valentini, N. Santillo, C. Petrucci, D. Lanari, E. Petricci, M. Taddei and L. Vaccaro, *ChemCatChem* 2018, **10**, 1277–1281.

37. A. Castellan, J.C.J. Bart and S. Cavallaro, *Catal. Today* 1991, **9**, 237–254.

38. T. Asano, M. Tamura, Y. Nakagawa and K. Tomishige, *ACS Sustainable Chem. Eng.* 2016, **4**, 6253–6257.

39. M.J. Gilkey, A. V. Mironenko, D.G. Vlachos and B. Xu, *ACS Catal.* 2017, **7**, 6619–6634.

40. M.J. Gilkey, R. Balakumar, D.G. Vlachos and B. Xu, *Catal. Sci. Technol.* 2018, **8**, 2661–2671.

41. L. Wei, J. Zhang, W. Deng, S. Xie, Q. Zhang and Y. Wang, *Chem. Commun.* 2019, **55**, 8013–8016.

42. G.M. Diamond, E.L. Dias, R. Archer, V.J. Murphy and T.R. Boussie, US Pat. 20160090346A1, 2016.

43. J. Lin, H. Song, X. Shen, B. Wang, S. Xie, W. Deng, D. Wu, Q. Zhang and Y. Wang, *Chem. Commun*., 2019, **55**, 11017–11020.

44. R.T. Larson, A. Samant, J. Chen, W. Lee, M.A. Bohn, D.M. Ohlmann, S.J. Zuend and F.D. Toste, *J. Am. Chem. Soc.* 2017, **139**, 14001–14004.

45. N. Shin, S. Kwon, S. Moon, C.H. Hong and Y.G. Kim, *Tetrahedron* 2017, **73**, 4758–4765.

46. H. Zhang, X. Li, X. Su, E.L. Ang, Y. Zhang and H. Zhao, *ChemCatChem* 2016, **8**, 1500–1506.

47. X. Li, D. Wu, T. Lu, G. Yi, H. Su and Y. Zhang, *Angew. Chem. Int. Ed*. 2014, **53**, 4200–4204.

48. M. Shiramizu and F.D. Toste, *Angew. Chem. Int. Ed.* 2013, **52**, 12905–12909.

49. N.-Z. Xie, H. Liang, R.-B. Huang and P. Xu, *Biotechnol. Adv.* 2014, **32**, 615–622.

50. E. Skoog, J.H. Shin, V. Saez-Jimenz, V. Mapelli and L. Olsson, *Biotechnol. Adv.* 2018, **36**, 2248–2263.

View Article Online
DOI: 10.1039/D0GC01277G

51. A. Marckwordt, F. El Ouahabi, H. Amani, S. Tin, N.V. Kalevaru, P.C.J. Kamer, S. Wohlrab and J.G. de Vries, *Angew. Chem. Int. Ed.* 2019, **58**, 3486–3490.

52. J.G. de Vries, *Chem. Rec.* 2016, **16**, 2787–2800.

53. J.D. Nobbs, N.Z.B. Zainal, J. Tan, E. Drent, L.P. Stubbs, C. Li, S.C.Y. Lim, D.G.A. Kumbang and M. van Meurs, *ChemstrySelect* 2016, **3**, 539–544.

54. P. Meesssen, D. Vogt and W. Keim, *J. Organomet. Chem.* 1998, **551**, 165–170.

55. D. Wu, Z. Chen, Z. Jia and L. Shuai, *Sci. Chin. Chem.* 2012, **55**, 380–385.

56. Y. Yang, X. Wei, F. Zeng and L. Deng, *Green Chem.* 2016, **18**, 691–694.

57. L. El Aakel, F. Launay, A. Atlamsani and J.-M. Brégeault, *Chem. Commun.* 2001, 2218–2219.

58. L. El Aakel, F. Launay, J.-M. Brégeault and A. Atlamsani, *J. Mol. Catal. A* 2004, **212**, 171–182.

59. M. Vennat, P. Herson, J.-M. Brégeault and G.B. Shul'pin, *Eur. J. Inorg. Chem.* 2003, 908–917.

60. E. Rozhko, K. Raabova, F. Macchia, A. Malmusi, P. Righi, P. Accorinti, S. Alini, P. Babini, G. Cerrato, M. Manzoli and F. Cavani, *ChemCatChem* 2013, **5**, 1998–2008.

61. N. Obara, Y. Nakagawa, M. Tamura and K. Tomishige, *ChemCatChem,* 2016, **8**, 1732–1738.

62. Y. Nakagawa, D. Sekine, N. Obara, M. Tamura and K. Tomishige, *ChemCatChem*, 2017, **9**, 3412–3419.

63. I.V. Kozhevnikov, *Chem. Rev.* 1998, **98**, 171–198.

64. N. Mizuno and M. Misono, *Chem. Rev.* 1998, **98**, 199–218.

65. W. Trakarnpruk and J. Jatupisarnpong, *Appl. Petrochem. Res.* 2013, **3**, 9–15.

66. R. Wçlfel, N. Taccardi, A. Bçsmann and P. Wasserscheid, *Green Chem.* 2011, **13**, 2759–2763.

67. J. Albert, R. Wçlfel, A. Bçsmann and P. Wasserscheid, *Energy Environ. Sci.* 2012, **5**, 7956–7962.

68. J. Li, D.-J. Ding, L. Deng, Q.-X. Guo and Y. Fu, *ChemSusChem* 2012, **5**, 1313–1318.

69. Z. Tang, W. Deng, Y. Wang, E. Zhu, X. Wan, Q. Zhang and Y. Wang, *ChemSusChem* 2014, **7**,

View Article Online
DOI: 10.1039/D0GC01277G

1557–1567.

70. J. Zhang, M. Sun, X. Liu and Y. Han, *Catal. Today* 2014, **233**, 77–82.

71. W. Wang, M. Niu, Y. Hou, W. Wu, Z. Liu, Q. Liu, S. Ren and K.N. Marsh, *Green Chem.* 2014, **16**, 2614–2618.

72. M. Niu, Y. Hou, S. Ren, W. Wang, Q. Zheng and W. Wu, *Green Chem.* 2015, **17**, 335–342.

73. M. Niu, Y. Hou, S. Ren, W. Wu and K.N. Marsh, *Green Chem.* 2015, **17**, 453–459.

74. T. Lu, M. Niu, Y. Hou, W. Wu, S. Ren and F. Yang, *Green Chem.* 2016, **18**, 4725–4732.

75. H. Weiner and R.G. Finke, *J. Am. Chem. Soc.* 1999, **121**, 9831–9842.

76. C.-X. Yin and R.G. Finke, *J. Am. Chem. Soc.* 2005, **127**, 13988–13996.

77. A.M. Morris, C.G. Pierpont and R.G. Finke, *J. Mol. Catal. A* 2009, **309**, 137–145.

78. S.K. Hanson, R.T. Baker, J.C. Gordon, B.L. Scott and D.L. Thorn, *Inorg. Chem.* 2010, **49**, 5611–5618.

79. S.K. Hanson, R. Wu and L.A. Silks, *Angew. Chem. Int. Ed.* 2012, 51, 3410–3413; *Angew. Chem.* 2012, **124**, 3466 –3469.

80. B. Sedai, C. Díaz-Urrutia, R.T. Baker, R. Wu, L.A. Silks and S.K. Hanson, *ACS Catal.* 2011, **1**, 794–804.

81. Y. Ma, Z. Du, J. Liu, F. Xia and J. Xu, *Green Chem.* 2015, **17**, 4968–4973.

82. J. Mottweiler, M. Puche, C. Räuber, T. Schmidt, P. Concepcijn, A. Corma and C. Bolm, *ChemSusChem* 2015, **8**, 2106–2113.

83. Y.-Y. Jiang, L. Yan, H.-Z. Yu, Q. Zhang and Y. Fu, *ACS Catal.* 2016, **6**, 4399–4410.

84. J. Liu, Z. Du, Y. Yang, T. Lu, F. Lu and J. Xu, *ChemSusChem* 2012, **5**, 2151–2154.

85. J. Lan, J. Lin, Z. Chen and G. Yin, *ACS Catal.* 2015, **5**, 2035–2041.

86. I.A. Weinstock, R.E. Schreiber and R. Neumann, *Chem. Rev.* 2018, **118**, 2680−2717.

View Article Online
DOI: 10.1039/D0GC01277G

87. K. Prantz and J. Mulzer, *Chem. Rev.* 2010, **110**, 3741−3766.

88. A. Sorokin, S.D. Suzzoni-Dezard, D. Puyllain, J.-P. Noël and B. Meunier, *J. Am. Chem. Soc.* 1996, **118**, 7410−7411.

89. S. L. Kachkarova-Sorkina, P. Gallezot and A.B. Sorokin, *Chem. Commun.* 2004, 2844−2845.

90. H.F.T. Klare, A.F.G. Goldberg, D.C. Duquette and B.M. Stoltz, *Org. Lett.* 2017, **19**, 988−991.

View Article Online
DOI: 10.1039/D0GC01277G

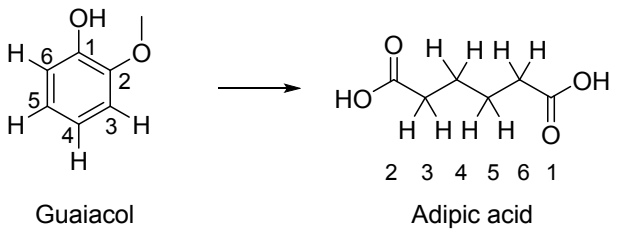

Scheme 1. Conversion of guaiacol to adipic acid.

View Article Online
DOI: 10.1039/D0GC01277G

Table 1. 2-MCO oxidation with various catalysts.

Entry	Catalyst (Amount/ μmol)	Reaction time /h	Conv. /%	Yield /%-C							AA sel. /%-C	Carbon balance /%
				AA	GA	SA	FA	MeOH	Others	CO_2		
1	Blank	24	7	1.9	0.2	<0.1	0.1	1.2	3.7	0.1	26	96
2	$H_5PV_2W_{10}O_{40}$ (55)	24	71	31	2.6	3.2	3.9	11	13	6.2	44	97
3	V_2O_5 (55)	24	31	11	1.4	1.9	1.8	3.9	7.0	3.6	37	105
4	V_2O_5 (55)	72	93	30	5.0	9.3	6.0	11	16	17	32	92
5	V_2O_5 (55) + $H_3PMo_{12}O_{40}$ (110)	24	77	46	0.8	0.5	1.2	11	14	3.1	60	100
6	V_2O_5 (55) + $H_3PW_{12}O_{40}$ (110)	24	79	36	1.9	1.6	2.7	11	21	5.8	45	98
7	V_2O_5 (55) + $H_4SiW_{12}O_{40}$ (110)	24	84	23	3.7	9.6	8.1	12	8.7	19	28	90
8	$H_4PVW_{11}O_{40}$ (110)	24	75	46	1.5	1.2	1.3	10	12	2.7	61	96
9	$H_3PW_{12}O_{40}$ (110)	24	60	45	1.1	0.2	0.4	9.7	3.8	0.2	74	97
10	$H_4SiW_{12}O_{40}$ (110)	24	38	21	1.0	0.3	0.7	7.9	5.9	0.8	56	108
11	H_2WO_4 (1320)	24	6	1.2	0.1	<0.1	0.7	1.3	2.8	0.3	19	98
12	H_2SO_4 (165)	24	18	8.2	0.6	0.1	0.2	2.9	5.4	0.2	46	96

Reaction conditions: 2-Methoxycyclohexanone (2-MCO) 4.3 mmol, catalyst 0-1320 μmol, water 10 g, O_2 0.8 MPa (at r. t.), 353 K, 24 or 72 h. AA: adipic acid, GA: glutaric acid, SA: succinic acid, FA: formic acid.

View Article Online
DOI: 10.1039/D0GC01277G

Table 2. Effect of O_2 pressure in 2-MCO oxidation with $H_3PW_{12}O_{40}$ catalyst.

Entry	O_2 pressure /MPa	Conv. /%	Yield /%-C								AA sel. /%-C	Carbon balance /%
			2-HCO	AA	GA	SA	FA	MeOH	Others	CO_2		
1	0.1	55	<0.1	40	0.4	0.1	0.2	6.8	6.9	0.1	73	95
2	0.3	56	<0.1	38	0.7	0.1	0.2	7.9	8.9	0.3	67	108
3	0.5	57	<0.1	41	1.1	0.2	0.4	8.1	6.1	0.4	72	103
4	0.8	60	<0.1	45	1.1	0.2	0.4	9.7	3.8	0.2	74	97
5	0 (N_2)	6	2.3	0.5	<0.1	<0.1	<0.1	1.2	1.8	0.1	8.5	96

Reaction conditions: 2-methoxycyclohexanone (2-MCO) 4.3 mmol, $H_3PW_{12}O_{40}$ 110 μmol, water 10 g, O_2 0.1-0.8 MPa (7-60 mmol) or N_2 0.8 MPa (at r. t.), 353 K, 24 h. 2-HCO: 2-hydroxycyclohexanone, AA: adipic acid, GA: glutaric acid, SA: succinic acid, FA: formic acid.

View Article Online
DOI: 10.1039/D0GC01277G

Table 3. Effect of reaction temperature in 2-MCO oxidation with $H_3PW_{12}O_{40}$ catalyst.

Entry	Temp. /K	Reaction time /h	Conv. /%	Yield /%-C							AA sel. /%-C	Carbon balance /%
				AA	GA	SA	FA	MeOH	Others	CO_2		
1	323	24	7	3.2	<0.1	<0.1	<0.1	1.1	2.3	<0.1	48	96
2	323	72	17	12	0.1	<0.1	0.1	2.5	2.4	0.1	70	96
3	353	24	60	45	1.1	0.2	0.4	9.7	3.8	0.2	74	97
4	353	120	98	74	2.8	0.5	1.0	13	6.1	1.2	75	94
5	383	24	>99	65	4.8	1.3	1.9	14	9.3	3.7	65	92

Reaction conditions: 2-methoxycyclohexanone (2-MCO) 4.3 mmol, $H_3PW_{12}O_{40}$ 110 μmol, water 10 g, O_2 0.8 MPa. AA: adipic acid, GA: glutaric acid, SA: succinic acid, FA: formic acid.

View Article Online
DOI: 10.1039/D0GC01277G

Table 4. Application to related substrates (cyclic compounds).

Entry	Substrate	Substrate amount /mmol	Conv. /%	Yield /%-C							Carbon balance /%
				AA	CHDO	GA	FA	MeOH	Others	CO_2	
1	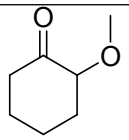 2-Methoxycyclohexanone (2-MCO)	4.3	60	45	<0.1	1.1	0.4	9.7	4.0	0.2	97
2	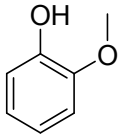 Guaiacol	4.3	1	<0.1	<0.1	<0.1	<0.1	<0.1	1.0	<0.1	93
3	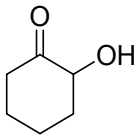 2-Hydroxycyclohexanone (2-HCO)	4.3	94	41	1.9	4.7	1.3	-	43	1.9	100
4		2.2	94	47	2.3	3.3	0.8	-	39	1.3	99
5		0.86	95	47	3.4	3.6	1.1	-	40	1.5	100
6	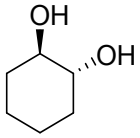 *trans*-1,2-Cyclohexanediol	4.3	1	<0.1	<0.1	<0.1	<0.1	-	0.7	0.1	107
7	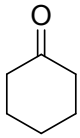 Cyclohexanone	4.3	2	<0.1	<0.1	<0.1	<0.1	-	2.0	<0.1	95
8	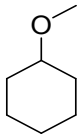 Methoxycyclohexane	4.3	3	<0.1	<0.1	<0.1	<0.1	0.5	2.8	<0.1	95

Reaction condition: substrate 0.86-4.3 mmol, $H_3PW_{12}O_{40}$ 110 μmol, water 10 g, O_2 0.8 MPa (at r. t.), 353 K, 24 h. AA: adipic acid, CHDO: 1,2-cyclohexanedione, GA: glutaric acid, FA: formic acid.

View Article Online
DOI: 10.1039/D0GC01277G

Table 5. Application to related substrates (acyclic compounds).

Entry	Substrate	Reaction time /h	Conv. /%	Yield /%-C						Carbon balance /%
				AcOH	FA	MeOH	2,3-Butanedione	Others	CO_2	
1	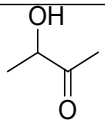 3-Hydroxy-2-butanone	24	59	48	0.2	-	10	1.2	0.1	104
2	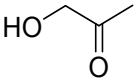 Hydroxyacetone	24	44	13	6.7	-	-	23	0.3	110
3	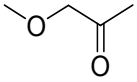	24	15	5.2	2.2	3.3	-	4.3	0.2	110
4	Methoxyacetone	72	38	14	6.7	7.8	-	8.6	0.6	105
5	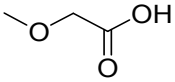 Methoxyacetic acid	24	1	-	<0.1	0.5	-	0.8	0.1	110

Reaction condition: substrate 4.3 mmol, $H_3PW_{12}O_{40}$ 110 μmol, water 10 g, O_2 0.8 MPa (at r. t.), 353 K, 24 or 72 h. AcOH: acetic acid, FA: formic acid.

View Article Online
DOI: 10.1039/D0GC01277G

Table 6. Effect of addition of radical inhibitor and catalyst reduction.

Entry	Catalyst	Additive	Conv. /%	Yield /%-C							AA sel. /%-C	Carbon balance / %
				AA	GA	SA	FA	MeOH	Others	CO_2		
1	Blank	-	7	1.9	0.2	<0.1	0.1	1.2	3.7	0.1	26	96
2	$H_3PW_{12}O_{40}$	-	60	45	1.1	0.2	0.4	9.7	3.8	0.2	74	97
3	$H_3PW_{12}O_{40}$	2.6-Di-*tert*-butyl-*p*-cresol	60	43	0.6	0.1	0.3	13	2.8	0.4	72	103
4	$H_{4.3}PW_{12}O_{40}$	-	62	43	1.5	0.3	0.5	8.1	8.1	0.5	69	102

Reaction condition: 2-methoxycyclohexanone (2-MCO) 4.3 mmol, catalyst 110 μmol, 2,6-di-*tert*-butyl-*p*-cresol 0 or 0.5 mmol, water 10 g, O_2 0.8 MPa (at r. t.), 353 K, 24 h. AA: adipic acid, GA: glutaric acid, SA: succinic acid, FA: formic acid.

View Article Online
DOI: 10.1039/D0GC01277G

Table 7. Calculated formation energy of radical cation from various molecules.

Molecule	ΔE /kJ mol^{-1}
2-Methoxycyclohexanone (2-MCO)	+797 (keto-form)
	+694 (enol-form)
Guaiacol	+745
Phenol	+804
Cyclohexanone	+867 (keto-form)
	+814 (enol-form)
2,6-Di-*tert*-butyl-*p*-cresol	+706

Calculation method: UB3LYP/6-311++G(d,p), gas phase, Gaussian 16 program package.

View Article Online
DOI: 10.1039/D0GC01277G

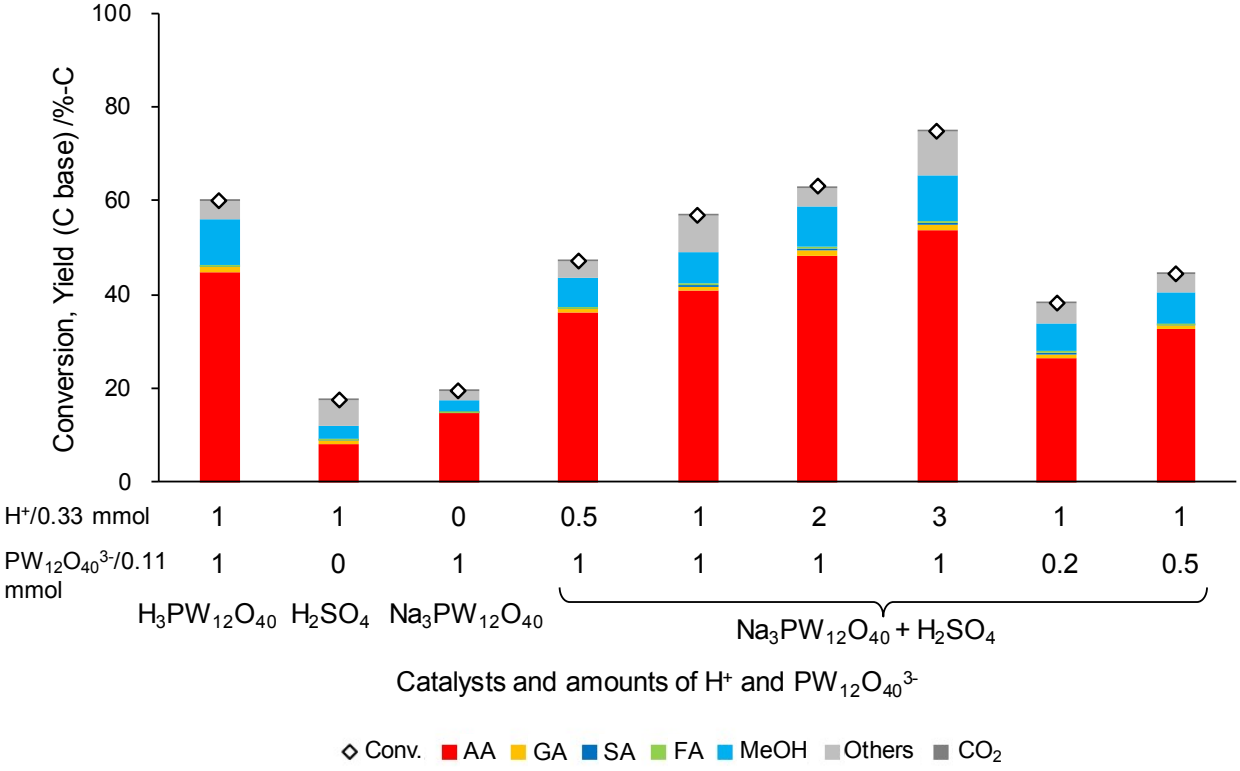

Fig. 1. Effect of ratio of $[H^+]$: $[PW_{12}O_{40}^{3-}]$ in 2-MCO oxidation.

Reaction condition: 2-methoxycyclohexanone (2-MCO) 4.3 mmol, $H_3PW_{12}O_{40}$ 110 μmol or $Na_3PW_{12}O_{40}$ 22-110 μmol, H_2SO_4 0-495 μmol, water 10 g, O_2 0.8 MPa (at r. t.), 353 K, 24 h. AA: adipic acid, GA: glutaric acid, SA: succinic acid, FA: formic acid.

View Article Online
DOI: 10.1039/D0GC01277G

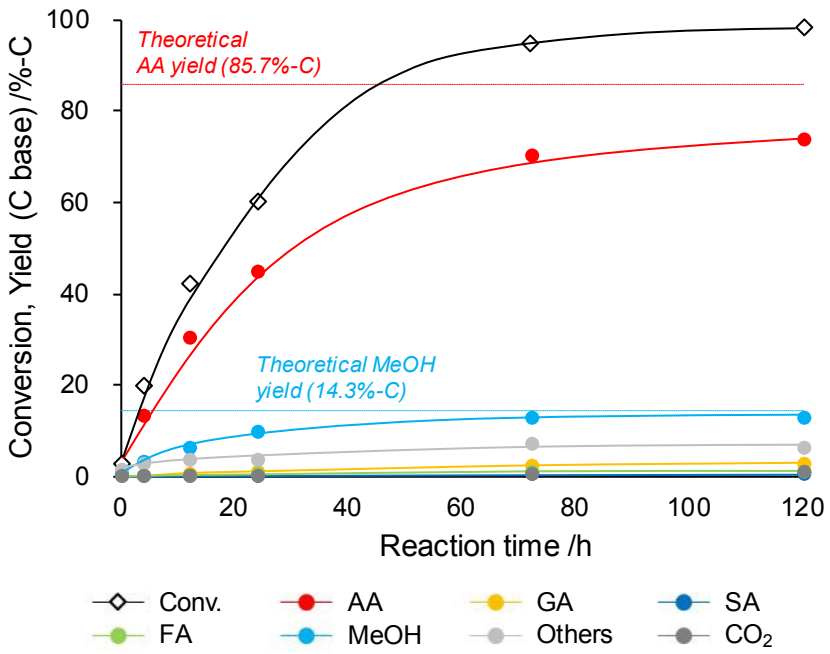

Fig. 2. Time course of the 2-MCO oxidation with $H_3PW_{12}O_{40}$ catalyst.

Reaction condition: 2-methoxycyclohexanone (2-MCO) 4.3 mmol, $H_3PW_{12}O_{40}$ 110 μmol, water 10 g, O_2 0.8 MPa (at r. t.), 353 K, 0-120 h. AA: adipic acid, GA: glutaric acid, SA: succinic acid, FA: formic acid.

View Article Online
DOI: 10.1039/D0GC01277G

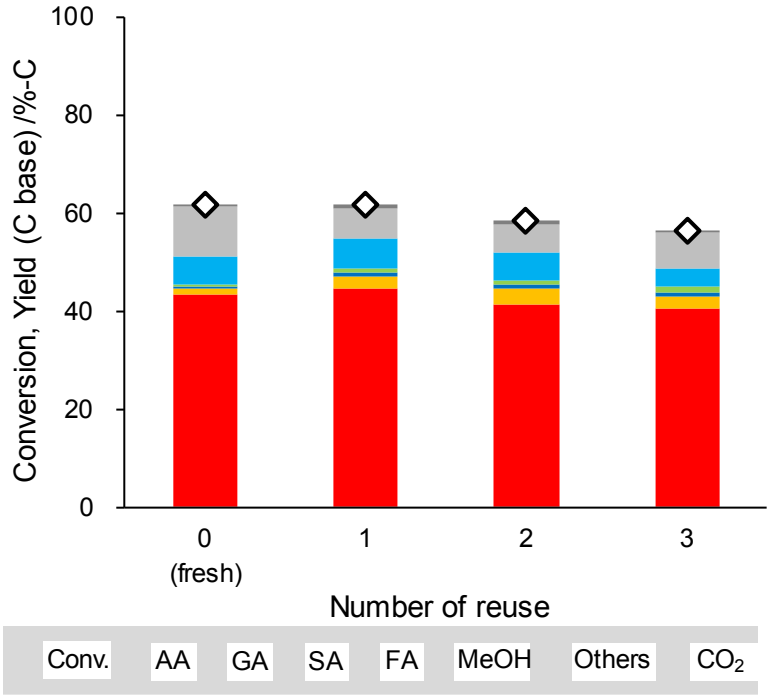

Fig. 3. Reusability of $H_3PW_{12}O_{40}$ catalyst in 2-MCO oxidation.

Reaction condition: 2-methoxycyclohexanone (2-MCO) 8.6 mmol (fresh), $H_3PW_{12}O_{40}$ 220 μmol (fresh), water 20 g (fresh), O_2 0.8 MPa (at r. t.), 353 K, 24 h. AA: adipic acid, GA: glutaric acid, SA: succinic acid, FA: formic acid.

View Article Online
DOI: 10.1039/D0GC01277G

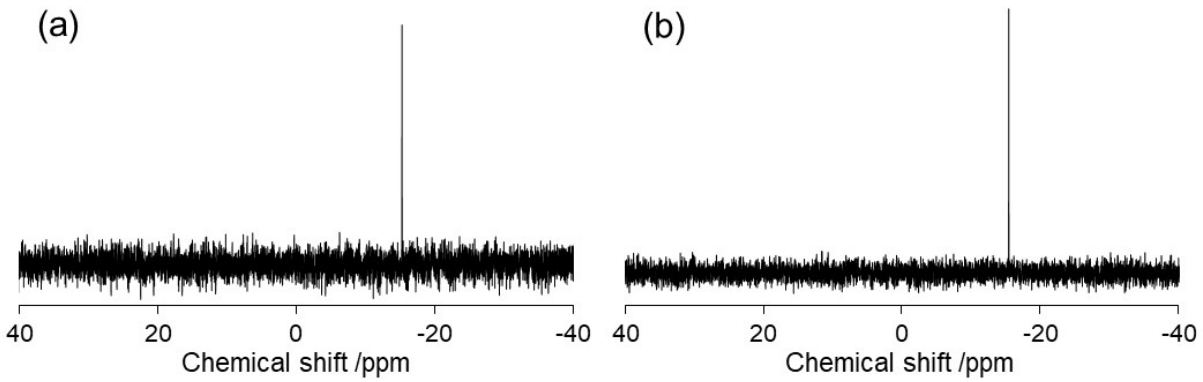

Fig. 4. ^{31}P NMR spectrum. (a) $H_3PW_{12}O_{40}aq$ (11 mmol/L). (b) Reaction solution after reuse experiment.

View Article Online
DOI: 10.1039/D0GC01277G

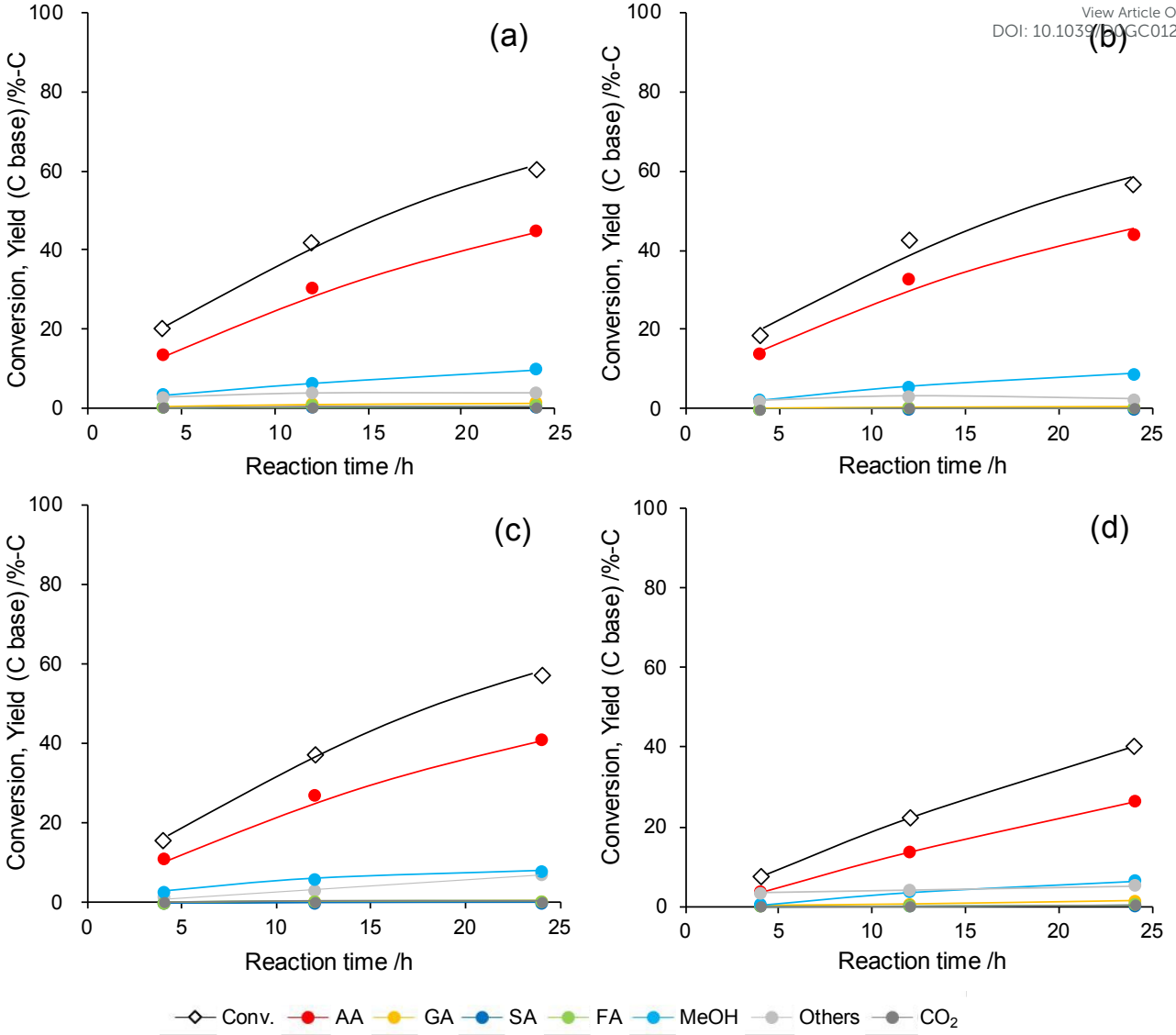

Fig. 5. Time course of the 2-MCO oxidation with $H_3PW_{12}O_{40}$ catalyst in different substrate concentration. (a) 2-MCO 4.3 mmol (standard). (b) 2-MCO 2.2 mmol. (c) 2-MCO 0.86 mmol. (d) 2-MCO 8.6 mmol.

Reaction condition: 2-methoxycyclohexanone (2-MCO) 0.86-8.6 mmol, $H_3PW_{12}O_{40}$ 110 μmol, water 10 g, O_2 0.8 MPa (at r. t.), 353 K, 4-12 h. AA: adipic acid, GA: glutaric acid, SA: succinic acid, FA: formic acid.

View Article Online
DOI: 10.1039/D0GC01277G

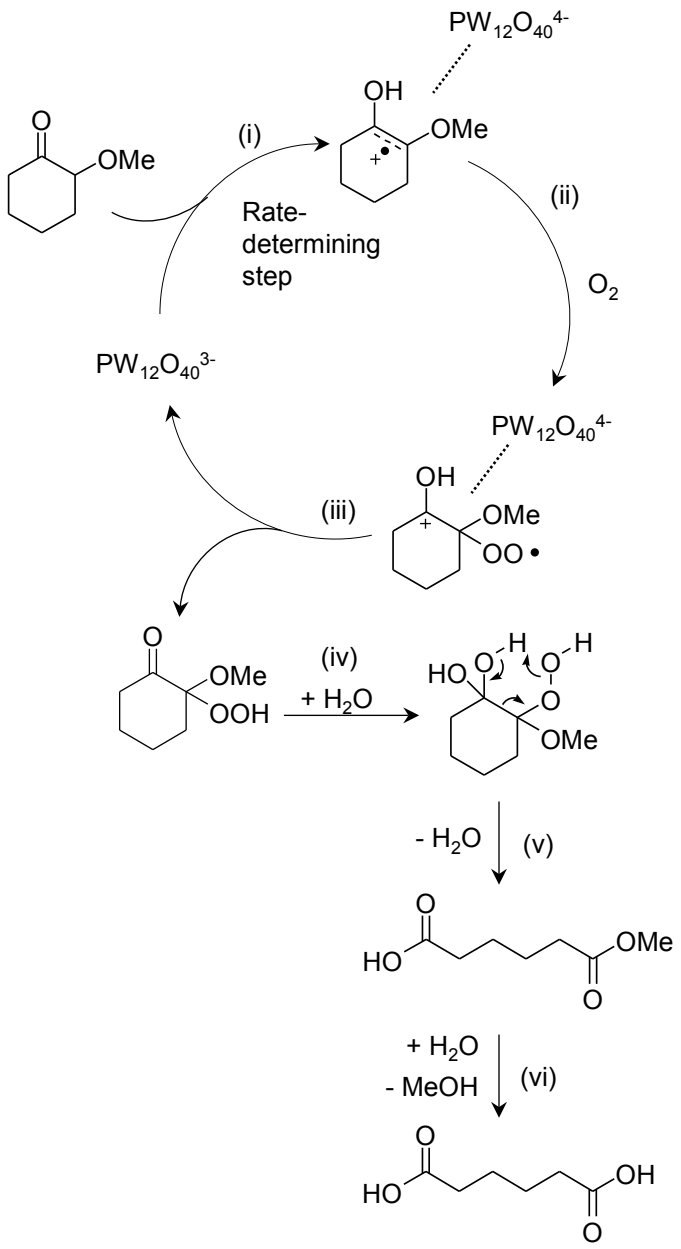

Fig. 6. Proposed reaction mechanism.

View Article Online
DOI: 10.1039/D0GC01277G

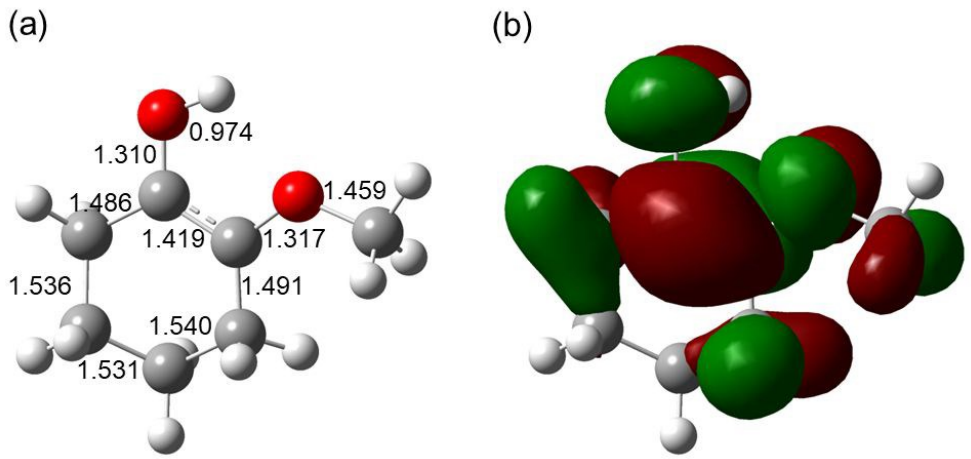

Fig. 7. Radical cation of 2-methoxycyclohexanone (enol form). (a) Calculated structure. Lengths in angstrom. (b) Molecular orbital occupied by unpaired electron.

Calculation method: UB3LYP/6-311++G(d,p), gas phase, Gaussian 16 program package.

Graphical abstract

View Article Online
DOI: 10.1039/D0GC01277G

Stable $H_3PW_{12}O_{40}$ catalyst can selectively convert 2-methoxycyclohexanone to adipic acid and methanol with O_2 as an oxidant in water.